Synthesis of Au-Cu Nano-Alloy from Monometallic Colloids by Simultaneous Pulsed Laser Targeting and Stirring

Mansoureh Ganjali*,   Monireh Ganjali,   Soraia Khoby,   Mohammad Ali Meshkot

Abstract: Experimental work has been focused on the formation of alloyed Au-Cu nanoparticles under simultaneous laser exposure and mechanical stirring of mixed monometallic colloids, here referred to as dual procedure. As a feed for the dual procedure, Au and Cu monometallic nanoparticle colloids have been using a laser ablation technique. To accomplish this, bulk targets were ablated with 1064 nm wavelength Nd: YAG laser in a pure acetone (99.99%) environment. Ultraviolet-visible optical absorption spectrometry, transmission electron microscopy, X-ray diffraction and X-ray fluorescence technique have been used to characterize the nanoparticles. It has been found that experimental conditions such as stirring and laser parameters strongly affect the synthesized particle properties, including the size, shape, composition and stability of the nanoparticles. Alloy nanoparticles containing 39% Au – 61% Cu have also been prepared in the same process, but in two forms of a homogeneous alloy and a core-shell structure.

Keywords: Laser ablation; Alloyed Au-Cu nanoparticles; Dual procedure; Laser exposure; Mechanical mixing; Core-shell

Introduction

In recent years, bimetallic nanoparticles (NPs) have gained much attention due to their applications as catalysts [1-3], in electro-optics [4] and for changes in surface plasma band energy [5,6]. Their shape, size, composition, crystallinity and structure can influenced by the experimental conditions during the preparation [7]. To produce NPs, different physical methods and combination techniques have been reported to date. Specific advantages of laser ablation technique (LAT) are its simplicity and versatility [8,9], well controlled exposure time [9], and the creation of pure NPs from colloidal dispersions with no formation of by-products [10]. On the other hand, colloids produced by chemical methods are usually contaminated with residual by-products such as ions and reducing agents, which is especially critical in biological applications [11]. In addition, LAT has been used for preparing various NPs such as noble metals [12], alloys [13,14], oxides [15] and semiconductors [16]. In submerged LAT, a laser beam ablates an immersed solid target at the liquid- solid surface [17]. In doing so, numerous novel possibilities could be reliably realized to create unique experimental conditions. These include laser parameters (wavelength, pulse duration, energy per pulse), ambient gas pressure and target distance. Such parameters can be used to control the shape and size distribution of the NPs [18]. NPs of Ag and Cu have been produced in many liquids [19,20]. LAT with a single or double pulsed laser has been used to obtain metallic alloy NPs of Au-Ag and Ag-Cu in colloids in several contexts [21].

Nanotechnology and Advanced Materials Department, Material and Energy Research Center, P. O. Box Tehran 14155-4777, Iran
*Corresponding author. E-mail: mansourehg@merc.ac.ir

In the present investigation, synthesis of gold and copper NPs from bulk targets by the LAT and Au-Cu bimetallic core-shell NPs by a dual procedure (DP) in acetone has been accomplished. DP can be used as an optimized method for the production of alloyed bimetallic NPs, using a low power density laser while magnetically stirring monometallic colloids at 200 rpm. The alloyed structures contain core-shell and homogeneous alloy formations.

Methods

A pulsed Nd:YAG laser with a near infra-red wavelength of 1064 nm and operated at 10 Hz was used as the ablation source. Each pulse had duration of 10ns and fluence of 5 J·cm^{-2} to ablate bulk targets normal to their surface. Gold and copper cube shaped targets of 1 cm^3 each and 99.99% purity were vigorously cleaned before the experiments. In the case of copper,

a complete surface layer was removed by laser ablation while it was submerged in acetone and then washed by deionized water and acetone in order to have a fresh metal surface. In the case of gold, cleaning was done several times at room temperature using a solution of KI:I$_2$:H$_2$O in the ratio 4 g:1 g:40 ml and ultrasound, followed by rinsing with deionized water and acetone.

Figure 1 shows four stages of the experimental setup. In stage 1, a gold target was ablated in acetone while stirring the medium to form gold nanoparticles. It should be noted that the acetone purity of 99.99% and freshness was of particular importance. Pure acetone was used throughout the experiments due to its lack of interaction with the laser beam. In stage 2 the size of gold nanoparticles was reduced further by removing the bulk target to leave the gold NPs colloid as the target. A similar setup with a copper target was used at stages 3 and 4 to form nanoparticles of copper. Throughout stages 1-4 the pulse width was 10 ns and the fluence was 5 J·cm^{-2}.
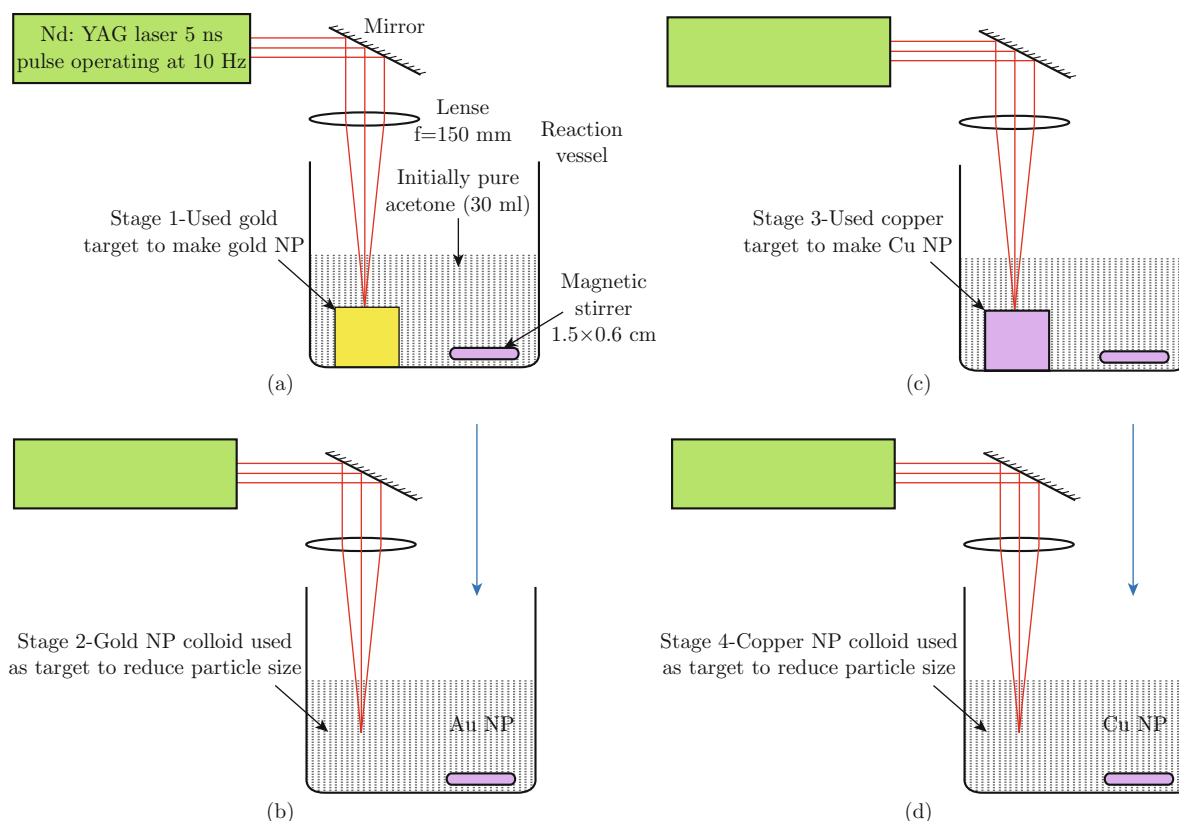

Fig. 1   Showing the experimental setup – stage 1: making gold nanoparticles; stage 2: reducing the size of AU NPs by laser treatment; stage 3: making copper nanoparticles; and stage 4: reducing Cu NPs colloid particle size.

In stages 5 and 6 (Fig. 2) the NP colloids produced in stages 2 and 4 were mixed in equal volume and stirred for various durations while being irradiated by the same laser but with a lower energy density of 0.3 J·cm^{-2} to produce Au-Cu alloy NPs.

Copper is reported to be highly reactive with respect to vapor from surrounding liquids [22,23]. Therefore all experiments were carries out in acetone to avoid oxidation of copper NPs and because acetone is transparent to the 1064 nm laser wavelength used.
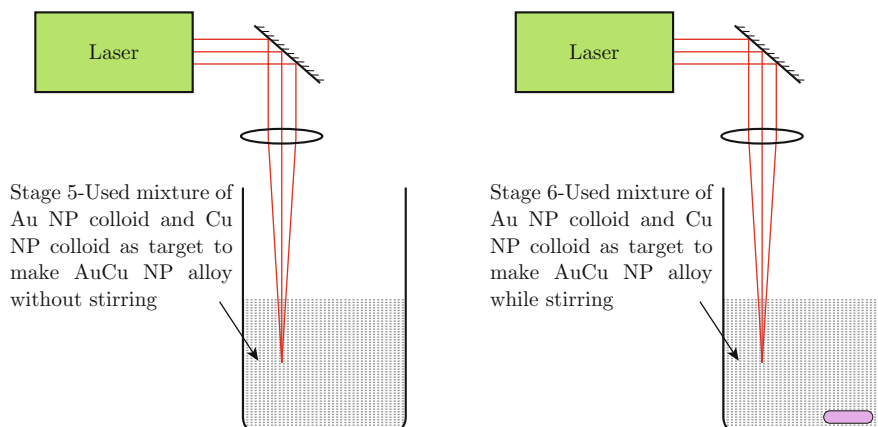
Fig. 2   Using an equal volume mixture of monometallic NP colloids from stages 2 and 4 to make Au-Cu alloy NPs with and without stirring.

Sample Preparation

In order to obtain NP samples for characterization from low concentration colloids, typically 5 and 16 mg of Cu and Au respectively in 30 ml of acetone, the colloids were kept at $5\pm2°C$ to avoid agglomeration and added dropwise over 7 days to a cylindrical 0.3 ml sample holder. The resulting samples were used for characterization. TEM samples were prepared in a similar way, but in this case the sample holder was a carbon coated copper grid. Indented silica slides were used to prepare X-ray diffraction (XRD) and X-ray fluorescence (XRF) samples. The XRD diffraction was carried out using a Philips PW3710 and transmission electron microscopy (TEM) observations (morphology and transmission electron diffraction TED pattern) were performed using a LEO912AB at 120 keV.

Optimization

A number of experimental parameters were optimized in order to achieve homogenous colloid concentrated NPs using a stabilized laser source. First, the laser beam was meticulously adjusted to produce near Gaussian beam during the exposure as shown in Fig. 3.
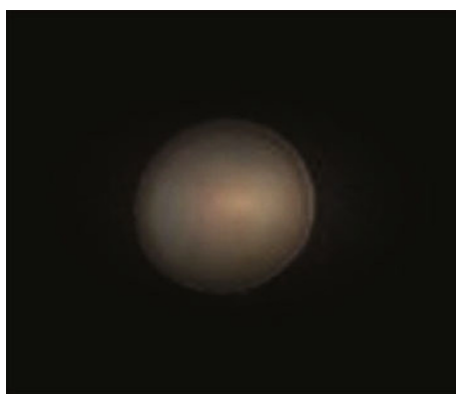

Fig. 3   Laser beam profile during exposure – near Gaussian.

Second, the beam power was measured against voltage to ensure the experiments were carried out in the linear region shown in Fig. 4. Thus the beam power during experiments was kept between 2.5 to 3 Watts.
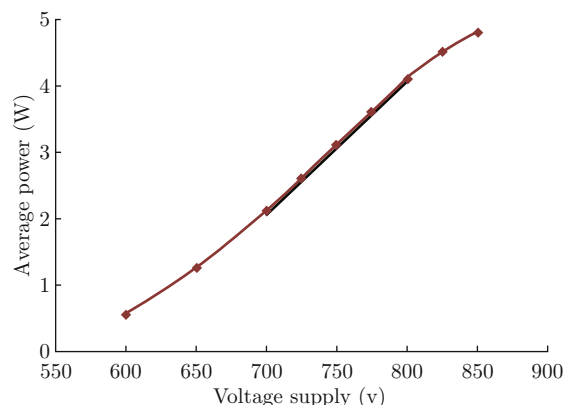

Fig. 4   Variation of laser output power with voltage was determined in order to ensure experiments were carried out in the linear region.

Third, the concentration of copper NPs was measured against the rotation speed of the magnetic stirrer as shown in Fig. 5, which shows the optimal stirring speed to be 200 rpm. Fourth, the copper NP concentration was measured at various beam fluency as shown in Fig. 6 to determine the optimum voltage/fluence combination. The colloid spectral absorbance was taken to be a measure of NP concentration. Finally the effect of duration of combined irradiation and stirring at stage 4 shown in Fig. 1 was investigated to determine its influence on the Cu NP concentration, see Fig. 7. Absorbance at the blue end of the spectrum was increased with longer irradiation due to the reduction in Cu NP size.
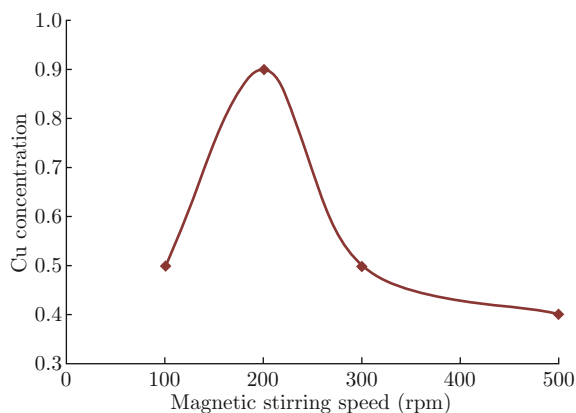
Fig. 5 Variation in the concentration of copper NPs as the stirring speed is changed.
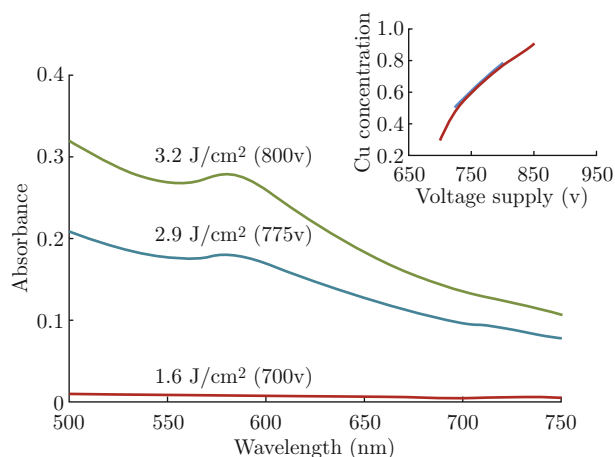

Fig. 6 Absorption spectra of Cu colloids synthesized by LAT in acetone on the various laser fluencies.
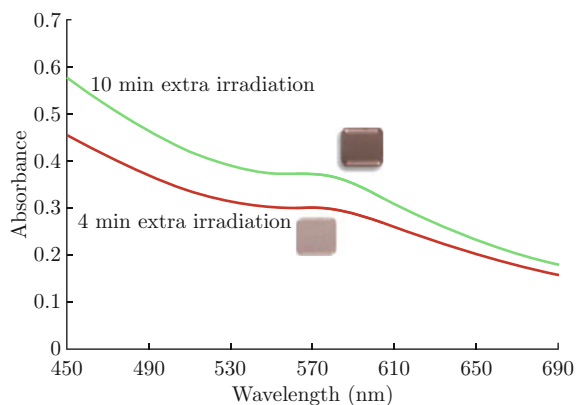

Fig. 7 Variation of NP concentration, taken to be proportional to spectral absorption, with durations of combined stirring and irradiation at stage 4 of Fig. 1.

Results and Discussion

During the ablation of the bulk targets (stage 1 and 3), it has been found that 5 minutes of ablation produced 15 mg of Au NPs in stage 1 and 5 mg of Cu NPs in stage 3. It has been observed that the acetone

remains transparent. The color of the solution gradually changes from light to dark after laser ablation starts. For example the color of the Au solution initially changes to light pink and then finally to dark purple. Even in the absence of a surfactant, the Au NP colloid prepared in acetone is stable for 18 months. Meanwhile, it has been reported that Cu NPs are chemically active and can easily react with vapors of surrounding liquid and any oxygen dissolved in the colloidal solution [24]. However, the 10 ns pulse of the laser beam is considered to be insufficient time for copper NPs to combine with any dissociated/dissolved oxygen. The synthesized Cu NPs are found to be stable in acetone without any sedimentation for a week at room temperature.

A magnetic stirrer has been used to produce a circulating and uniform colloid. Figure 5 shows that increasing the stirrer speed to 200 rpm at stage 3 results in the highest Cu NP concentration in the colloid, but further increase results in a decrease in concentration. It is believed to be likely that there are 2 competing processes when the laser beam of 5 J/cm^2 is directed into a liquid containing alloy-forming metal NPs of 5-7 nm at room temperature (Fig. 1). One process is that NPs within the beam path will split into smaller NPs. Another process is that NPs not in the beam path will collide and join to form larger particles; thereby reduce the NP concentration. Below 200 rpm the first process is considered to be dominant; whereas with stirring beyond 200 rpm, higher instances of collision between NPs is likely and the second process becomes dominant and hence the absorption intensity is reduced.

To further reduce the size of NPs, the NP colloids were further subjected to 30 minutes of the laser beam at stages 2 and 4 while stirring magnetically at the optimum speed of 200 rpm (Fig. 1(b) and (d)).

In one step of the experiments, the effect of the laser voltage on synthesized particles was investigated. A typical absorption spectrum of a Cu colloidal dispersion obtained by the LAT of bulk Cu in pure acetone under various laser fluencies are presented in Fig. 6. The inset of this figure shows that the relationship between Cu NP concentration and the laser fluence is not linear. In order to achieve higher colloidal stability, the current study has been performed in the linear region of the inset. The presence of a single surface plasmon peak indicates that the formed NPs were nearly spherical. In the case of the ellipsoidal particles the absorption spectrum would have two plasmon peaks [25-27].

The optical spectrum shows a relative maximum at about 582 nm, which is the plasmon absorption of the Cu NPs [24]. The intensity of the plasmon band increases in concurrence with increase of the laser voltage directly. In addition, it is noted that higher voltages cause the Cu NPs to oxidize and as a result the color of the prepared colloid turns gray brown.

Figure 8 shows the TEM images of Au and Cu NPs

produced by the ablation of corresponding metal targets in acetone medium after the particle size reduction of stages 2 and 4 of Fig. 1. According to this figure, the average size of Au and Cu NPs are about 5 nm and 7 nm, respectively. Moreover the images show the presence of nearly spherical particles.

Formation of the Au–Cu alloys

During stages 5 and 6 (Fig. 2) Au-Cu alloy NPs were formed, both as core-shell alloys as shown in the inset to TEM micrograph of Fig. 9(a) and as homogeneous alloy as determined by XRD pattern of Fig. 10. A low
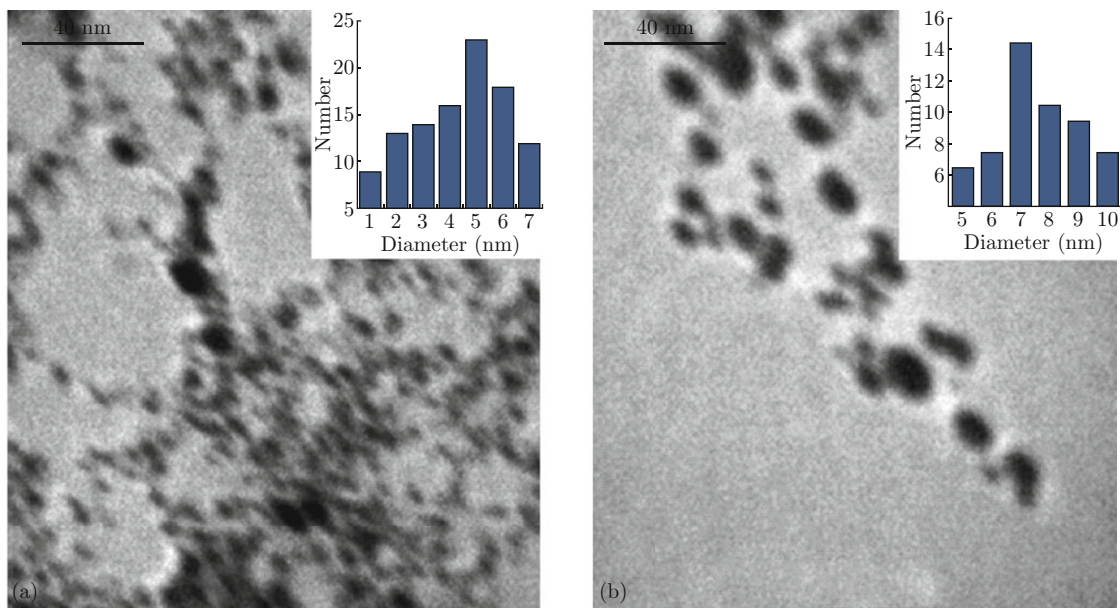

Fig. 8   TEM image of Gold (left) and Copper (right) nanoparticles with insets showing the particle size distribution as diameter (nm) against count.
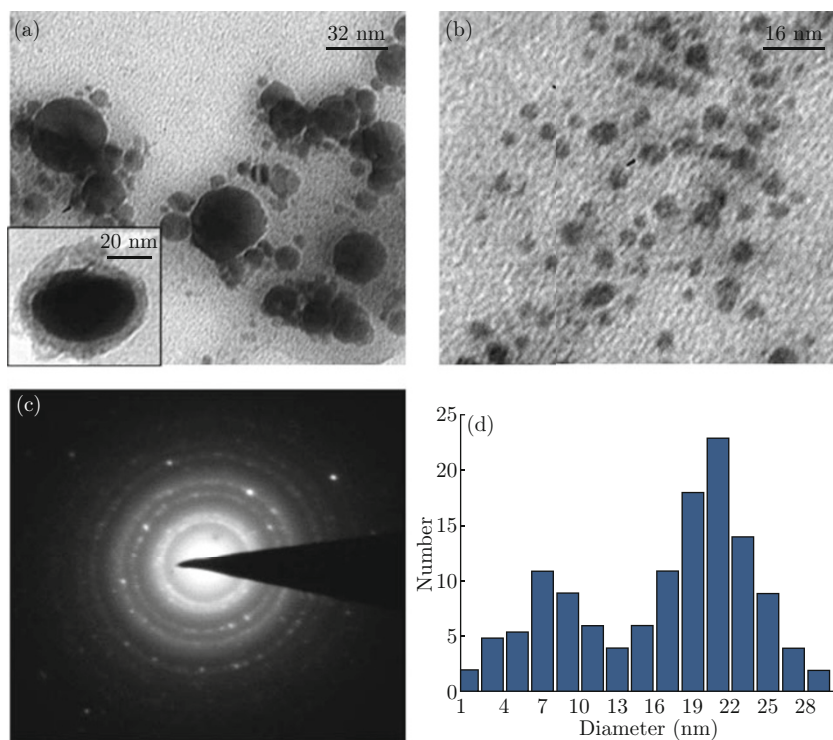

Fig. 9   AuCu alloy NPs made by laser irradiation of colloid mixture containing Au and Cu NPs. (a) and (b) show TEM image of alloy NPs and inset shows core-shell structure, (c) shows electron diffraction pattern and (d) shows size distribution.
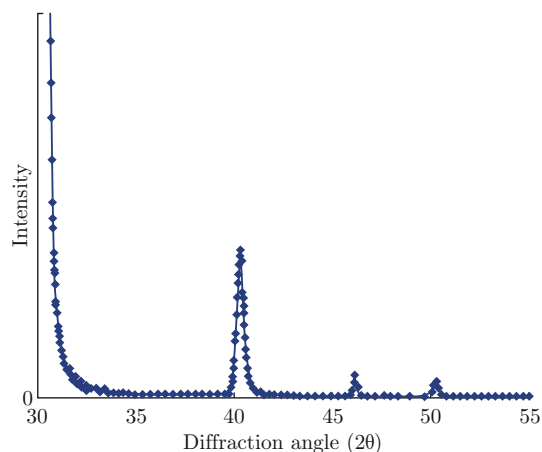
Fig. 10   X-ray diffraction pattern of AuCu alloy formed at stages 5 and 6 of figure 2.

energy density of 0.3 J·cm^{-2} was used at stages 5 and 6 with and without concurrent stirring. During stage 5 the vessel was turned by hand during 10 minutes of irradiation to enable fairly even irradiation of the liquid throughout. At stage 6, a magnetic stirrer was used at 200 rpm and resulted in more alloy NPs being produced in half the time. Therefore mixing during irradiation has a significant effect on the amount of alloy nanoparticles formed per unit time.

In the core-shell bimetallic structure, the dark nucleus corresponds to the initial Au NPs as a core, and the lighter layer relates to the Cu coating as a shell. As expected, there was great contrast between the Au and the Cu NPs because of the atomic mass difference. The Au-Cu NPs have almost spherical shapes. Formation of the core-shell NPs can be explained by considering a preferential condensation and nucleation of the small Cu NPs on large enough Au NPs in order to minimize the interfacial free energy.

The corresponding NPs size distribution for the TEM images also exhibits the bimodal size distribution with diameters of 7 and 20 nm. The TED pattern shows diffuse rings of the Au-Cu alloy NPs, indicating that the prepared NPs are well crystallized. Thus laser ablation in contrast to chemical techniques provides an easy, one step procedure for obtaining crystallized NPs without any post-process heat-treatments.

The absorption spectra of Au-Cu alloyed NPs were obtained immediately after irradiation and are presented in Fig. 11. The Au colloidal NPs exhibit a well defined absorption peak at 480 nm, which consist of the gold metal particles with sizes in the nanometer range. The Cu colloid also shows an absorption band near 582 nm, which indicates the production of copper colloids with sizes in the nanometer range. After mixing the Au and Cu colloids in equal volume (as mixed sample), the ultra violet-visible (UV-Vis) absorption spectra shows a double plasmon peak at around 480 and 580 nm, (not shown for the sake of brevity), indicating the pres-

ence of the pure gold and the copper NPs respectively. Thereafter the individual Au and Cu plasmon peaks disappear and a new peak is observed which suggests that alloying has occurred. In other words the position of plasmon frequency of an Au-Cu alloy is in between the maxima of the plasmon resonance of Au and Cu respectively. In comparing the two alloy curves, the one with stirring (DP) has higher absorption intensity than the hand-turned version. This is explained by the increased probability of having different single-metal NPs in the beam focus point at the same time.
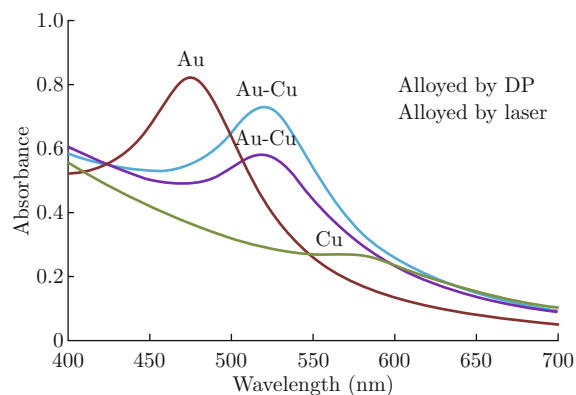

Fig. 11   UV-Vis absorption spectra for single metal and AuCu alloy produced by laser irradiation of a mixture of single-element colloids containing Au and Cu respectively. More alloys were formed in half the time when the colloid mixture was stirred during irradiation.

It is expected that the use of pure un-oxidized Cu to prepare the Au-Cu alloy would be a better choice because even small amounts of surface oxidation were found to cause agglomeration of Cu NPs and widening of the plasmon peak. Furthermore, oxides would be eliminated from the final alloy.

The Au-Cu alloy has a FCC structure, but the main process used for alloy formation on individual Au and Cu nanoparticle colloids at stage 6 results in the preparation of non-stoichiometric Au_xCu_{1-x} NPs. The mean composition of Au can be estimated using the d-spacing of crystallographic planes. Due to a very small Bragg angle in this case, the equation of Bragg's Law [28] can be simplified as Eqn. (1):

$$\lambda = 2d\theta \qquad (1)$$

But according to the geometry of a TEM, for a small Bragg angle Eqn. (2) applies,

$$2\theta = Lr \qquad (2)$$

where r is the path difference between the diffracted and the non-diffracted points and L is the camera length. Combining the above two relationships we have Eqn. (3):

$$L\lambda = rd \qquad (3)$$

The d-spacing of the alloy structure was obtained from Eqn. (3), where λ is the wavelength of the TEM electron beam which was 0.38 nm, L is the length of the camera, r is the radius of the diffraction pattern and d is the inter-planar spacing. The d-spacing was found to be 1.99 nm and the calculated lattice parameter from the TED pattern was calculated at 3.4468 nm which agrees well with the (111) set of planes, the highest density crystal plane of the FCC.

The mean value for (x) in the alloy composition was calculated from the Eqn. (4) [29].

$$a_{alloy} = xa_{Au} + (1-x)a_{Cu} + 0.01198x(1-x) \quad (4)$$

where a_{Au} = 4.08 nm and a_{Cu} = 3.61 nm, which are the Au and the Cu lattice parameters respectively. The mean composition of $Au_xCu_{(1-x)}$ was found to be $Au_{0.39}Cu_{0.61}$ which gives the Au-Cu ratio of 1.6. This is in agreement with the XRF result (Fig. 12).
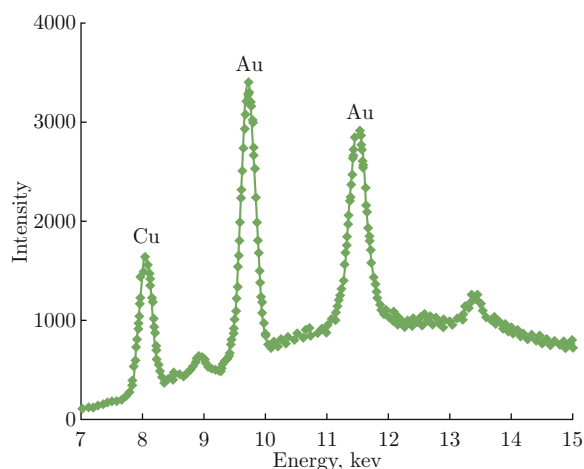

Fig. 12   XRF pattern for Au-Cu nanoalloy produced at stage 6.

For the dominant homogeneous alloy structure, the diffraction pattern of Figure 10 was recorded over a 2Θ range of 30-70° in steps of 0.02°. Due to the weak diffraction intensity of the Au-Cu synthesized NPs, XRD pattern at low bimetallic alloy concentration took a total scan time of 16 hours. Figure 10 exhibits three distinct diffraction peaks at 2Θ values of 40.4°, 45.7° and 49.8°, which correspond to the (111), (200) and (002) crystallographic planes of the tetragonal FCC Au-Cu as reported on JCPDS card 025-1220. The peak at 30° is related to the SiO_2 substrate.

Conclusions

In this investigation, the formation of Au-Cu alloy nanoparticles has been achieved through the application of a dual process of laser irradiation and simultaneous stirring of a mixture of single-metal colloids.

Stirring has been found to increase the alloy production rate. The individual Au and Cu colloids have a nano-particle size range of 1-7 and 5-12 nm respectively. In order to ensure stability, accuracy and repeatability, synthesis of the mono and bimetallic nano-particles are carried out after several calibration steps to ensure equal conditions at each stage. Stable colloids have been obtained lasting up to one year without agglomeration. Results show that the Au-Cu alloy nano-particles have both a core-shell structure as well as a more dominant homogeneous alloy structure. The plasmon band in the optical absorption spectrum of the Au-Cu alloy colloid appears as a peak between those of individual Au and Cu colloids.

The dual procedure for nano-alloy preparation described in this work offers flexibility, versatility, ease of use and cost effectiveness in bi- and multi-metallic alloy synthesis. For example, numerous opportunities can be exploited in the catalyst industry both to improve conventional materials as well as to create novel structures.

Acknowledgment

References

[1] N. Toshima, T. Yonezawa and K. Kushihashi, J. Chem. Soc. 89, 2537 (1993).

[2] K. Esumi, M. Wakabayashi and K. Torigoe, Colloids Surf. 109, 55 (1996). http://dx.doi.org/10.1016/0927-7757(95)03451-X

[3] L. M. Liz-Manzan and A. P. Philipe, J. Phys. Chem. 99, 15120 (1995). http://dx.doi.org/10.1021/j100041a031

[4] G. Schon and U. Simon, Colloid Polym. Sci. 273, 202 (1995). http://dx.doi.org/10.1007/BF00657826

[5] S. W Han, Y. Kim and K. Kim, J. Colloid Interf. Sci. 208, 272 (1998). http://dx.doi.org/10.1006/jcis.1998.5812

[6] S. Link, Z. L. Wang and M. A. El-Sayed, J. Phys. Chem. B 103, 3529 (1999). http://dx.doi.org/10.1021/jp990387w

[7] X. P. Zhu, Tsuneo Suzuki, Tadachika Nakayama, Hisayuki Suematsu, Weihua Jiang and Koichi Niihara, Chem. Phys. Lett. 427, 127 (2006). http://dx.doi.org/10.1016/j.cplett.2006.05.119

[8] M. Saito, K. Yasukawa, T. Umeda and Y. Aoi, Opt. Mater. 30, 1201 (2008). http://dx.doi.org/10.1016/j.optmat.2007.05.049

[9] N. V. Tarasenko, V. S. Burakov and A. V. Butsen, Astron. Obs. Belgrade, 201 (2007).

[10] Physics, Chemistry and Application of Nanostructures: review and short notes to Nanomeeting 2003: Minsk, Belarus 17-21 May 2003, World Scientific Publishing Co Pte. Ltd, Minsk (2003).

[11] N. V. Tarasenko, A. V. Butsen, E. A. Nevar and N. A. Savastenko, Appl. Surf. Sci. 252, 4439 (2006). http://dx.doi.org/10.1016/j.apsusc.2005.07.150

[12] H. J. Kim, I. C. Bang and J. Onoe, Opt. Laser. Eng. 47, 532 (2009). http://dx.doi.org/10.1016/j.optlaseng.2008.10.011

[13] Z. WG and J. ZG, Sci. Chin. Ser. B, 47 159 (2004).

[14] S. H. Sun, C. B. Murray, D. Weller, L. Folks and A. Moser, Science 287, 1989 (2000). http://dx.doi.org/10.1126/science.287.5460.1989

[15] R. K. Thareja and S. Shukla, Appl. Surf. Sci. 253, 8889 (2007). http://dx.doi.org/10.1016/j.apsusc.2007.04.088

[16] R. A. Ganeev and A. I. Ryasnyansky, Opt. Commun. 246, 163 (2005). http://dx.doi.org/10.1016/j.optcom.2004.10.056

[17] G. W. Yang, Prog. Mater. Sci. 52, 648 (2007). http://dx.doi.org/10.1016/j.pmatsci.2006.10.016

[18] J. C. Alonso, R. Diamant, P. Castillo, M. C. Acosta-Garcia, N. Batina and E. Haro-Poniatowskiet, Appl. Surf. Sci. 255, 4933 (2009). http://dx.doi.org/10.1016/j.apsusc.2008.12.040

[19] T. Tsuji, K. Iryo, N. Watanabe and M. Tsuji, Appl. Surf. Sci. 202, 80 (2002). http://dx.doi.org/10.1016/S0169-4332(02)00936-4

[20] T. Tsuji, T. Kakita and M. Tsuji, Appl. Surf. Sci. 206, 314 (2003). http://dx.doi.org/10.1016/S0169-4332(02)01230-8

[21] T. Tsuji, Y. Tsuboi, N. Kitamura and M. Tsuji, Appl. Surf. Sci. 229, 365 (2004). http://dx.doi.org/10.1016/j.apsusc.2004.02.013

[22] Kazuyuki Amikura, Takeshi Kimura, Mika Hamada, Noriko Yokoyama, Jun Miyazaki and Yasuhiro Yamada, Appl. Surf. Sci. 254, 6976 (2008). http://dx.doi.org/10.1016/j.apsusc.2008.05.091

[23] Lee Jaehoon, Kim Dong-Kuk and Kang Weekyung, Bull. Korean Chem. Soc. 27, 1869 (2006). http://dx.doi.org/10.5012/bkcs.2006.27.11.1869

[24] P. V. Kazakevich, A. Simakin, V. Voronov and G. Shafeev, Appl. Surf. Sci. 252, 4373 (2006). http://dx.doi.org/10.1016/j.apsusc.2005.06.059

[25] N. V. Tarasenko, A. V. Butsen, E. A. Nevar and N. A. Savastenko, Appl. Surf. Sci. 252, 4439 (2006). http://dx.doi.org/10.1016/j.apsusc.2005.07.150

[26] A. T. Izgaliev, A. V. Simakin and G. A. Shafeev, Quantum Electron. 34, 47 (2004). http://dx.doi.org/10.1070/QE2004v034n01ABEH002578

[27] G. Compagnini and R. S.Cataliotti, Appl. Surf. Sci. 254, 1007 (2007). http://dx.doi.org/10.1016/j.apsusc.2007.07.177

[28] Principles of Optics: Electromagnetic Theory of Propagation, Interference and Diffraction of Light 7th edition, Published by the Press Syndicate of the University of Cambridge (1999).

[29] H. Yasouda and H. Mori, Phys. Rev. Lett. 69, 37 (1992).